PointNet: Deep Learning on Point Sets for 3D Classification and Segmentation

Article · December 2016

CITATIONS
41

READS
827

4 authors, including:

Charles Ruizhongtai Qi
Stanford University
11 PUBLICATIONS **332** CITATIONS
SEE PROFILE

Hao Su
Stanford University
58 PUBLICATIONS **5,420** CITATIONS
SEE PROFILE

Kaichun Mo
Stanford University
2 PUBLICATIONS **42** CITATIONS
SEE PROFILE

PointNet: Deep Learning on Point Sets for 3D Classification and Segmentation

Anonymous CVPR submission

Paper ID 201

Abstract

Point cloud is an important type of geometric data structure. Due to its irregular format, most researchers transform such data to regular 3D voxel grids or collections of images. This, however, renders data unnecessarily voluminous and causes issues. In this paper, we design a novel type of neural network that directly consumes point clouds, which well respects the permutation invariance of points in the input. Our network, named PointNet, provides a unified architecture for applications ranging from object classification, part segmentation, to scene semantic parsing. Though simple, PointNet is highly efficient and effective. Empirically, it shows strong performance on par or even better than state of the art. Theoretically, we provide analysis towards understanding of what the network has learnt and why the network is robust with respect to input perturbation and corruption.

1. Introduction

In this paper we explore deep learning architectures capable of reasoning about 3D geometric data such as point clouds or meshes. Typical convolutional architectures require highly regular input data formats, like those of image grids or 3D voxels, in order to perform weight sharing and other kernel optimizations. Since point clouds or meshes are not in a regular format, most researchers typically transform such data to regular 3D voxel grids or collections of images (e.g, views) before feeding them to a deep net architecture. This data representation transformation, however, renders the resulting data unnecessarily voluminous — while also introducing quantization artifacts that can obscure natural invariances of the data.

For this reason we focus on a different input representation for 3D geometry using simply point clouds – and name our resulting deep nets *PointNets*. Point clouds are simple and unified structures that avoid the combinatorial irregularities and complexities of meshes, and thus are easier to learn from. The PointNet, however, still has to respect the fact that a point cloud is just a set of points and therefore invariant to permutations of its members, necessitating certain symmetrizations in the net computation. Further invariances to rigid motions also need to be considered.

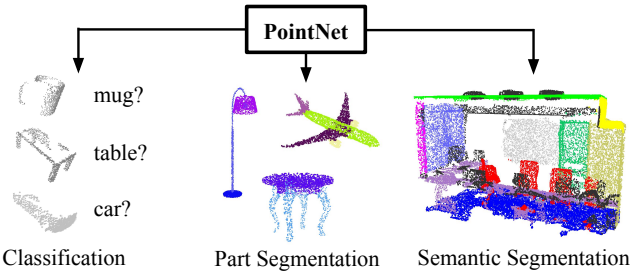

Figure 1. Applications of PointNet. We propose a novel deep net architecture that consumes raw point cloud (set of points) without voxelization or rendering. It is a unified architecture that learns both global and local point features, providing a simple, efficient and effective approach for a number of 3D recognition tasks.

Our PointNet is a unified architecture that directly takes point clouds as input and outputs either class labels for the entire input or per point segment/part labels for each point of the input. The basic architecture of our network is surprisingly simple as in the initial stages each point is processed identically and independently. In the basic setting each point is represented by just its three coordinates (x, y, z). Additional dimensions may be added by computing normals and other local or global features.

Key to our approach is the use of a single symmetric function, max pooling. Effectively the network learns a set of optimization functions/criteria that select interesting or informative points of the point cloud and encode the reason for their selection. The final fully connected layers of the network aggregate these learnt optimal values into the global descriptor for the entire shape as mentioned above (shape classification) or are used to predict per point labels (shape segmentation).

Our input format is easy to apply rigid or affine transfor-

mations to, as each point transforms independently. Thus we can add a data-dependent spatial transformer network that attempts to canonicalize the data before the PointNet processes them, so as to further improve the results.

We provide both a theoretical analysis and an experimental evaluation of our approach. We show that our network can approximate any set function that is continuous. More interestingly, it turns out that our network learns to summarize an input point cloud by a sparse set of key points, which roughly corresponds to the skeleton of objects according to visualization. The theoretical analysis provides an understanding why our PointNet is highly robust to small perturbation of input points as well as to corruption through point insertion (outliers) or deletion (missing data).

On a number of benchmark datasets ranging from shape classification, part segmentation to scene segmentation, we experimentally compare our PointNet with state-of-the-art approaches based upon multi-view and volumetric representations. Under a unified architecture, not only is our PointNet much faster in speed, but it also exhibits strong performance on par or even better than state of the art.

The key contributions of our work are as follows:

- We design a novel deep net architecture suitable for consuming unordered point sets in 3D;
- We show how such a net can be trained to perform 3D shape classification, shape part segmentation and scene semantic parsing tasks;
- We provide thorough empirical and theoretical analysis on the stability and efficiency of our method;
- We illustrate the 3D features computed by the selected neurons in the net and develop intuitive explanations for its performance.

The problem of processing unordered sets by neural nets is a very general and fundamental problem – we expect that our ideas can be transferred to other domains as well.

2. Related Work

Point Cloud Features Most existing features for point cloud are handcrafted towards specific tasks. Point features often encode certain statistical properties of points and are designed to be invariant to certain transformations, which are typically classified as intrinsic [2, 21, 3] or extrinsic [18, 17, 13, 10, 5]. They can also be categorized as local features and global features. For a specific task, it is not trivial to find the optimal feature combination.

Deep Learning on 3D Data 3D data has multiple popular representations, leading to various approaches for learning. *Volumetric CNNs:* [25, 15, 16] are the pioneers applying 3D convolutional neural networks on voxelized shapes. However, volumetric representation is constrained by its resolution due to data sparsity and computation cost of 3D convolution. FPNN [12] and Vote3D [23] proposed special methods to deal with the sparsity problem; however, their operations are still on sparse volumes, it's challenging for them to process very large point clouds. *Multiview CNNs:* [20, 16] have tried to render 3D point cloud or shapes into 2D images and then apply 2D conv nets to classify them. With well engineered image CNNs, this line of methods have achieved dominating performance on shape classification and retrieval tasks [19]. However, it's nontrivial to extend them to scene understanding or other 3D tasks such as point classification and shape completion. *Spectral CNNs:* Some latest works [4, 14] use spectral CNNs on meshes. However, these methods are currently constrained on manifold meshes such as organic objects and it's not obvious how to extend them to non-isometric shapes such as furniture. *Feature-based DNNs:* [6, 8] firstly convert the 3D data into a vector, by extracting traditional shape features and then use a fully connected net to classify the shape. We think they are constrained by the representation power of the features extracted.

Deep Learning on Unordered Sets From a data structure point of view, a point cloud is an unordered set of vectors. While most works in deep learning focus on regular input representations like sequences (in speech and language processing), images and volumes (video or 3D data), not much work has been done in deep learning on point sets.

One recent work from Oriol Vinyals et al [22] looks into this problem. They use a read-process-write network with attention mechanism to consume unordered input sets and show that their network has the ability to sort numbers. However, since their work focuses on generic sets and NLP applications, there lacks the role of geometry in the sets.

3. Problem Statement

We design a deep learning framework that directly consumes unordered point sets as inputs. A point cloud is represented as a set of 3D points $\{P_i| \ i = 1, ..., n\}$, where each point P_i is a vector of its (x, y, z) coordinate plus extra feature channels such as color, normal etc. For simplicity and clarity, unless otherwise noted, we only use the (x, y, z) coordinate as our point's channels.

For the object classification task, the input point cloud is either directly sampled from a shape or pre-segmented from a scene point cloud. Our proposed deep network outputs k scores for all the k candidate classes. For semantic segmentation, the input can be a single object for part region segmentation, or a sub-volume from a 3D scene for object region segmentation. Our model will output $n \times m$ scores for each of the n points and each of the m semantic subcategories.

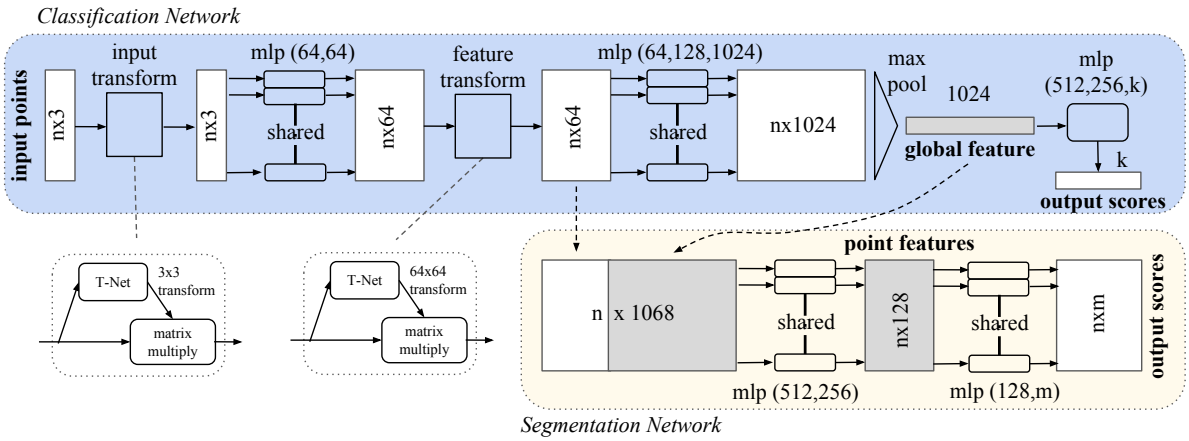

Figure 2. PointNet Architecture. The classification network takes n points as input, applies input and feature transformations, and then aggregates point features by max pooling. The output is classification score for k classes. The segmentation network is an extension to the classification net. It concatenates global and local features and outputs per point scores. "mlp" stands for multi-layer perceptron, the numbers in bracket are its layer sizes. Batchnorm is used for all layers with ReLU. Dropout layers are used for the last mlp in classification net.

4. Deep Learning on Point Sets

The architecture of our network (Sec 4.2) is inspired by the properties of point sets in $\mathbb{R}^n$ (Sec 4.1).

4.1. Properties of Point Sets in $\mathbb{R}^n$

Our input is a subset of points from an Euclidean space. It has three main properties:

- Unordered. Unlike pixel arrays in images or voxel arrays in volumetric grids, point cloud is a set of points without specific order in the points. In other words, a network that consumes N 3D point sets needs to be invariant to $N!$ permutations of the input set in data feeding order.
- Interaction among points. The points are from a space with a distance metric. It means that points are not isolated, and neighboring points form a meaningful subset. Therefore, the model needs to be able to capture local structures from nearby points, and the combinatorial interactions among local structures.
- Invariance under transformations. As a geometric object, the learned representation of the point set should be invariant to certain transformations. For example, rotating and translating points all together should not modify the global point cloud category nor the segmentation of the points.

4.2. PointNet Architecture

Our full network architecture is visualized in Fig 2, where the classification network and the segmentation network share a great portion of structures. Please read the caption of Fig 2 for the pipeline.

Our network has three key modules: the max pooling layer as a symmetric function to aggregate information from all the points, a local and global information combination structure, and two joint alignment networks that align both input points and point features.

We will discuss our reason behind these design choices in separate paragraphs below.

Symmetry Function for Unordered Input In order to make a model invariant to input permutation, three strategies exist: 1) sorting input into a canonical order; 2) treat the input as a sequence to train an RNN, but augment the training data by all kinds of permutations; 3) use a simple symmetric function to aggregate the information from each point. Here, a symmetric function takes n vectors as input and outputs a new vector that is invariant to the input order. For example, $+$ and $*$ operators are symmetric binary functions.

While sorting sounds like a simple solution, in high dimensional space there in fact does not exist an ordering that is stable w.r.t. point perturbations in the general sense. This can be easily shown by contradiction. If such an ordering strategy exists, it defines a bijection map between a high-dimensional space and a $1d$ real line. It is not hard to see, to require an ordering to be stable w.r.t point perturbations is equivalent to requiring that this map preserves spatial proximity as the dimension reduces, a task that cannot be achieved in the general case. Therefore, sorting does not fully resolve the ordering issue, and it's hard for a network to learn a consistent mapping from input to output as the ordering issue persists. As shown in experiments (Fig 5), we find that applying a MLP directly on the sorted point set performs poorly, though slightly better than directly processing an unsorted input.

The idea to use RNN considers the point set as a sequential signal and hopes that by training the RNN

with randomly permuted sequences, the RNN will become invariant to input order. However in "OrderMatters" [22] the authors have shown that order does matter and cannot be totally omitted. While RNN has relatively good robustness to input ordering for sequences with small length (dozens), it's hard to scale to thousands of input elements, which is the common size for point sets. Empirically, we have also shown that model based on RNN does not perform as well as our proposed method (Fig 5).

Our idea is to approximate a general function defined on a point set by applying a symmetric function on transformed elements in the set:

$$f(\{x_1, \ldots, x_n\}) \approx g(h(x_1), \ldots, h(x_n)), \qquad (1)$$

where $f : 2^{\mathbb{R}^N} \to \mathbb{R}$, $h : \mathbb{R}^N \to \mathbb{R}^K$ and $g : \underbrace{\mathbb{R}^K \times \cdots \times \mathbb{R}^K}_{n} \to \mathbb{R}$ is a symmetric function.

Empirically, our basic module is very simple: we approximate h by a multi-layer perceptron network and g by a composition of a single variable function and a max pooling function. This is found to work well by experiments. Through a collection of h, we can learn a number of f's to capture different properties of the set.

While our key module seems simple, it has interesting properties (see Sec 5.3) and can achieve strong performace (see Sec 5.1) in a few different applications. Due to the simplicity of our module, we are also able to provide theoretical analysis as in Sec 4.3.

Local and Global Information Aggregation The output from the above section forms a vector $[f_1, \ldots, f_K]$, which is a global signature of the input set. We can easily train a SVM or multi-layer perceptron classifier on the shape global features for classification. However, point segmentation requires a combination of local and global knowledge. We can achieve this by a simple yet highly effectively manner.

Our solution can be seen in Fig 2 (*Segmentation Network*). After computing the global point cloud feature vector, we feed it back to per point features by concatenating the global feature with each of the point features. Then we extract new per point features based on the combined point features - this time the per point feature is aware of both the local and global information.

With this modification our network is able to predict per point quantities that rely on both local geometry and global semantics. For example we can accurately predict per-point normals (fig in supplementary), validating that the network is able to summarize information from the point's local neighborhood. In experiment session, we also show that our model can achieve state-of-the-art performance on shape part segmentation and scene segmentation.

Joint Alignment Network The semantic labeling of a point cloud has to be invariant if the point cloud undergoes certain geometric transformations, such as rigid transformation. We therefore expect that the learnt representation by our point set is invariant to these transformations.

A natural solution is to align all input set to a canonical space before feature extraction. Jaderberg et al. [9] introduces the idea of spatial transformer to align 2D images through sampling and interpolation, achieved by a specifically tailored layer implemented on GPU.

Our input form of point clouds allows us to achieve this goal in a much simpler way compared with [9]. We do not need to invent any new layers and no alias is introduced as in the image case. We predict an affine transformation matrix by a mini-network and directly apply this transformation to the coordinates of input points. The mini-network itself resembles the big network and is composed by basic modules of point independent feature extraction, max pooling and fully connected layers.

This idea can be further extended to the alignment of feature space, as well. We can insert another alignment network on point features and predict a feature transformation matrix to align features from different input point clouds. However, transformation matrix in the feature space has much higher dimension than the spatial transform matrix, which greatly increase the difficulty of optimization. We therefore add a regularization term to our softmax training loss. We constraint the feature transformation matrix to be close to orthogonal matrix:

$$L_{reg} = \|I - AA^T\|_F^2, \qquad (2)$$

where A is the feature alignment matrix predicted by a mini-network. An orthogonal transformation will not lose information in the input, thus is desired. We find that by adding the regularization term, the optimization becomes more stable and our model achieves better performance.

4.3. Theoretical Analysis

Universal approximation We first show the universal approximation ability of our neural network to continuous set functions. By the continuity of set functions, intuitively, a small perturbation to the input point set should not greatly change the function values, such as classification or segmentation scores.

Formally, let $\mathcal{X} = \{S : S \subseteq [0,1]^m\}$, $f : \mathcal{X} \to \mathbb{R}$ is a continuous set function on $\mathcal{X}$ w.r.t to Hausdorff distance $d_H(\cdot,\cdot)$, i.e., $\forall \epsilon > 0, \exists \delta > 0$, for any $S, S' \in \mathcal{X}$, if $d_H(S, S') < \delta$, then $|f(S) - f(S')| < \epsilon$. Our theorem says that f can be arbitrarily approximated by our network given enough neurons at the max pooling layer, i.e., K in (1) is sufficiently large.

Theorem 1. *Suppose $f : \mathcal{X} \to \mathbb{R}$ is a continuous set function w.r.t Hausdorff distance $d_H(\cdot,\cdot)$. $\forall \epsilon >$*

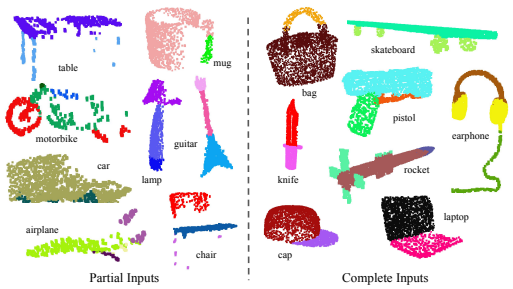

Figure 3. Qualitative results for part segmentation. We visualize the CAD part segmentation results across all 16 object categories. We show both results for partial simulated Kinect scans (left block) and complete ShapeNet CAD models (right block).

0, $\exists$ *a continuous function* h *and a symmetric function* $g(x_1, \ldots, x_n) = \gamma \circ MAX$*, such that for any* $S \in \mathcal{X}$*,*

$$\left| f(S) - \gamma \left(\underset{x_i \in S}{MAX} \{h(x_i)\} \right) \right| < \epsilon$$

where $x_1, \ldots, x_n$ *is the full list of elements in* S *ordered arbitrarily,* γ *is a continuous function, and MAX is a vector max operator that takes* n *vectors as input and returns a new vector of the element-wise maximum.*

The proof to this theorem can be found in our supplementary material. The key idea is that in the worst case the network can learn to convert a point cloud into a volumetric representation, by partitioning the space into equal-sized voxels. In practice, however, the network learns a much smarter strategy to probe the space, as we shall see in the experiment section.

Bottleneck dimension and stability Theoretically and experimentally we find that the expressiveness of our network is strongly affected by the dimension of the max pooling layer, i.e., K in (1). Here we provide an analysis, which also reveals properties related to the stability of our model.

We define $\mathbf{u} = \underset{x_i \in S}{MAX}\{h(x_i)\}$ to be the sub-network of f which maps a point set in $[0, 1]^m$ to a K-dimensional vector. The following theorem tells us that small corruptions or extra noise points in the input set is not likely to change the output of our network:

Theorem 2. *Suppose* $\mathbf{u} : \mathcal{X} \to \mathbb{R}^K$ *such that* $\mathbf{u} = \underset{x_i \in S}{MAX}\{h(x_i)\}$ *and* $f = \gamma \circ \mathbf{u}$*. Then,*

(a) $\forall S, \exists\, \mathcal{C}_S, \mathcal{N}_S \subseteq \mathcal{X}$*,* $f(T) = f(S)$ *if* $\mathcal{C}_S \subseteq T \subseteq \mathcal{N}_S$*;*

(b) $|\mathcal{C}_S| \leq K$

We explain the implications of the theorem. (a) says that $f(S)$ is unchanged up to the input corruption if all points in $\mathcal{C}_S$ are preserved; it is also unchanged with extra noise points up to $\mathcal{N}_S$. (b) says that $\mathcal{C}_S$ only contains a bounded number of points, determined by K in (1). In other words, $f(S)$ is in fact totally determined by a finite subset $\mathcal{C}_S \subseteq S$ of less or equal to K elements. We therefore call $\mathcal{C}_S$ the *critical point set* of S and K the *bottleneck dimension* of f.

Combined with the continuity of h, this explains the robustness of our model w.r.t point perturbation, corruption and extra noise points. The robustness is gained in analogy to the sparsity principle in machine learning models. **Intuitively, our network learns to summarize a shape by a sparse set of key points.** In experiment section we see that the key points form the skeleton of an object.

	input	#views	accuracy avg. class	accuracy overall
SPH [11]	mesh	-	68.2	-
3DShapeNets [25]	volume	1	77.3	84.7
VoxNet [15]	volume	12	83.0	85.9
Subvolume [16]	volume	20	86.0	**89.2**
LFD [25]	image	10	75.5	-
MVCNN [20]	image	80	**90.1**	-
Ours baseline	point	-	72.6	77.4
Ours PointNet	point	1	86.2	**89.2**

Table 1. Classification results on ModelNet40. Our net achieves state-of-the-art among deep nets on 3D input.

5. Experiment

Experiments are divided into three parts. First, we show PointNets can be applied to multiple 3D recognition tasks (Sec 5.1). Second, we provide detailed experiments to validate our network design (Sec 5.2). Third, we visualize what the network learns (Sec 5.3).

5.1. Applications

In this section we show how our network can be trained to perform 3D object classification, object part segmentation and semantic scene segmentation [1]. Even though we are working on a brand new data representation (point sets), we are able to achieve comparable or even better performance on benchmarks for several tasks.

3D Object Classification Our network learns global point cloud feature that can be used for object classification. We evaluate our model on the ModelNet40 [25] shape classification benchmark. There are 12,311 CAD models from 40 man-made object categories, split into 9,843 for training and 2,468 for testing. While previous methods focus on volumetric and mult-view image representations, we are the first to directly work on raw point cloud.

[1] More application examples such as correspondence and point cloud based CAD model retrieval are included in supplementary material.

	mean	aero	bag	cap	car	chair	ear phone	guitar	knife	lamp	laptop	motor	mug	pistol	rocket	skate board	table
# shapes		2690	76	55	898	3758	69	787	392	1547	451	202	184	283	66	152	5271
Wu [24]	-	63.2	-	-	-	73.5	-	-	-	74.4	-	-	-	-	-	-	74.8
Yi [26]	81.4	81.0	78.4	77.7	**75.7**	87.6	61.9	**92.0**	85.4	**82.5**	**95.7**	**70.6**	91.9	**85.9**	53.1	69.8	75.3
3DCNN	79.4	75.1	72.8	73.3	70.0	87.2	63.5	88.4	79.6	74.4	93.9	58.7	91.8	76.4	51.2	65.3	77.1
Ours	**83.7**	**83.4**	**78.7**	**82.5**	74.9	**89.6**	**73.0**	91.5	**85.9**	80.8	95.3	65.2	**93.0**	81.2	**57.9**	**72.8**	**80.6**

Table 2. Segmentation results on ShapeNet part dataset. Metric is mean IoU(%) across shapes. We compare with two traditional methods [24] and [26] and a 3D fully convolutional network baseline proposed by us. Our PointNet method achieved the state-of-the-art in mIoU.

We uniformly sample 1024 points on mesh faces according to face area. Points are normalized into a unit sphere with. During training we augment the point cloud on-the-fly by randomly rotating the object along the up-axis and jitter the position of each points by a Gaussian noise with zero mean and 0.02 standard deviation.

In Table 1, we compare our model with previous works as well as our baseline using MLP on traditional features extracted from point cloud (point density, D2, shape contour etc.). Our model achieved state-of-the-art performance among methods based on 3D input (volumetric and point cloud). With only fully connected layers and max pooling, our net gains a strong lead in inference speed and can be easily parallelized in CPU as well. There is still a small gap between our method and multi-view based method (MVCNN [20]), which we think is due to the loss of fine geometry details that can be captured by rendered images.

3D Object Part Segmentation Part segmentation is a challenging fine-grained 3D recognition task. Given a 3D scan or a mesh model, the task is to assign part category label (e.g. chair leg, cup handle) to each point or face.

We evaluate on ShapeNet part data set from [26], which contains 16,881 shapes from 16 categories, annotated with 50 parts in total. Most object categories are labeled with two to five parts. Ground truth annotations are labeled on sampled points on the shapes.

We formulate part segmentation task as a per-point classification problem. Evaluation metric is IoU on points for every part on a shape and mean IoU across shapes.

In this section, we compare our segmentation version PointNet (Fig 2, *Segmentation Network*) with two traditional methods [24] and [26] that both take advantage of point-wise geometry features and correspondences between shapes, as well as 3D CNN, a volumetric deep learning method. We design the segmentation 3D CNN architecture as a fully convolutional one that keeps volume size through all layers. In the end each voxel has a receptive field of 19 voxels with spatial resolution of 32. See the supplemental for the detailed network architecture.

In Table 2, we report per-category and mean IoU(%) scores. We observe a 2.3% mean IoU improvement and our net beats the baseline methods in most categories.

We also perform experiments on simulated Kinect scans to test the robustness of these methods. For every CAD model in the ShapeNet part data set, we use Blensor Kinect Simulator [7] to generate incomplete point clouds from six random viewpoints. We train our PointNet on the complete shapes and partial scans with the same network architecture and training setting. Results show that we lose only 5.3% mean IoU. In Fig 3, we present qualitative results on both complete and partial data. One can see that though partial data is fairly challenging, our predictions are reasonable.

Semantic Segmentation in Scenes Our network on part segmentation can be easily extended to semantic scene segmentation, where point labels become semantic object classes instead of object part labels.

We experiment on the Stanford 3D semantic parsing data set [1]. The dataset contains 3D scans from Matterport scanners in 6 areas including 271 rooms. Each point in the scan is annotated with one of the semantic labels from 13 categories (chair, table, floor, wall etc. plus clutter).

To prepare training data, we firstly split points by room, and then sample rooms into blocks with area 1m by 1m. We train our segmentation version of PointNet to predict per point class in each block. Each point is represented by a 9-dim vector of XYZ, RGB and normalized location as to the room (from 0 to 1). At training time, we randomly sample 4096 points in each block on-the-fly. At test time, we test on all the points. We follow the same protocol as [1] to use k-fold strategy for train and test.

	mean IoU	overall accuracy
Ours baseline	20.12	53.19
Ours PointNet	**47.71**	**78.62**

Table 3. Results on semantic segmentation in scenes. Metric is average IoU over 13 classes (structural and furniture elements plus clutter) and classification accuracy calculated on points.

	table	chair	sofa	board	mean
# instance	455	1363	55	137	
Armeni et al. [1]	46.02	16.15	**6.78**	3.91	18.22
Ours	**46.67**	**33.80**	4.76	**11.72**	**24.24**

Table 4. Results on 3D object detection in scenes. Metric is average precision with threshold IoU 0.5 computed in 3D volumes.

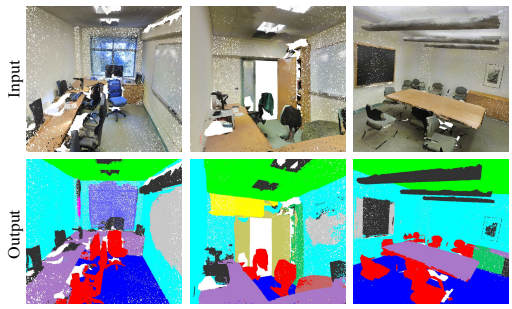

Figure 4. Qualitative results for semantic segmentation. Top row is input point cloud with color. Bottom row is output semantic segmentation result (on points) displayed in the same camera viewpoint as input.

We compare our method with a baseline using hand-crafted point features. The baseline extracts the same 9-dim local features and three additional ones: local point density, local curvature and normal. We use standard MLP as the classifier. Results are shown in Table 3, where our PointNet method significantly outperforms the baseline method. In Fig 4, we show qualitative segmentation results. Our network is able to output smooth predictions and is robust to missing points and occlusions.

Based on the semantic segmentation output from our network, we further build a 3D object detection system using connected component for object proposal (see supplementary for details). We compare with previous state-of-the-art method in Table 4. The previous method is based on a sliding shape method (with CRF post processing) with SVMs trained on local geometric features and global room context feature in voxel grids. Our method outperforms it by a large margin on the furniture categories reported.

5.2. Architecture Design Analysis

In this section we validate our design choices [2] by control experiments. We also show the effects of our network's hyperparameters.

Comparison with Alternative Order-invariant Methods As mentioned in Sec 4.2, there are at least three options for consuming unordered set inputs. We use the ModelNet40 shape classification problem as a test bed for comparisons of those options, the following two control experiment will also use this task.

The baselines (illustrated in Fig 5) we compared with include multi-layer perceptron on unsorted and sorted points as $n \times 3$ arrays, RNN model that considers input point as a sequence, and a model based on symmetry functions. The symmetry operation we experimented include max pooling, average pooling and an attention based weighted sum. The attention method is similar to that in [22], where a scalar score is predicted from each point feature, then the score is normalized across points by computing a softmax. The weighted sum is then computed on the normalized scores and the point features. As shown in Fig 5, max-pooling operation achieves the best performance by a large winning margin, which validates our choice.

[2] Due to the limit of space, we refer the analysis on bottleneck dimension and number of input points to supplementary.

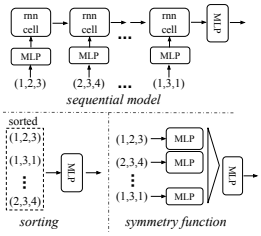

	accuracy
MLP (unsorted input)	24.2
MLP (sorted input)	45.0
LSTM	78.5
Attention sum	83.0
Average pooling	83.8
Max pooling	**87.1**

Figure 5. Three approaches to achieve order invariance. Multi-layer perceptron (MLP) applied on points consists of 5 hidden layers with neuron sizes 64,64,64,128,1024, all points share a single copy of MLP. The MLP close to the output consists of two layers with sizes 256. All fully connected layers are using ReLU and batch normalization (except the output layer). Two dropouts with keep prob 0.8 are applied to each hidden layer of the output MLP.

Effectiveness of Input and Feature Transformations In Table 5 we demonstrate the positive effects of our input and feature transformations (for alignment). It's interesting to see that the most basic architecture already achieves quite reasonable results. Using input transformation gives a 0.8% performance boost. The regularization loss is necessary for the higher dimension transform to work. By combining both transformations and the regularization term, we achieve the best performance.

Robustness Test We show our PointNet, while simple and effective, is robust to various kinds of input corruptions. We use the same architecture as in Fig 5's max pooling network. Input points are normalized into a unit sphere. Results are in Fig 6.

As to missing points, when there are 50% points missing, the accuracy only drops by 2.4% and 3.8% w.r.t. furthest and random input sampling. Our net is also robust to outlier points, if it has seen those during training. We evaluate two models: one trained on points with (x, y, z) coordinates; the other on (x, y, z) plus point density. The net has more than

Transform	accuracy
none	87.1
input (3x3)	87.9
feature (64x64)	86.9
feature (64x64) + reg.	87.4
both	**89.2**

Table 5. Effects of input feature transforms. Metric is overall classification accuracy on ModelNet40 test set.

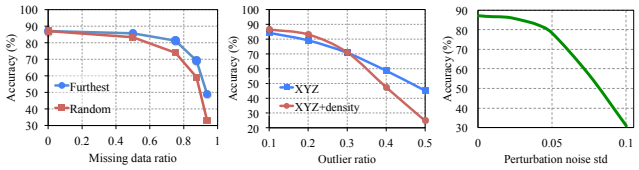

Figure 6. PointNet robustness test. The metric is overall classification accuracy on ModelNet40 test set. Left: Delete points. Furthest means the original 1024 points are sampled with furthest sampling. Middle: Insertion. Outliers uniformly scattered in the unit sphere. Right: Perturbation. Add Gaussian noise to each point independently.

80% accuracy even when 20% of the points are outliers. Fig 6 right shows the net is robust to point perturbations.

5.3. Visualizing PointNet

We design two experiments to visualize what has been learnt by the PointNet. The results are consistent with the theoretical analysis in Sec 4.3. In the first experiment, we visualize the learnt point function $h(x)$ in Eq 1, which demonstrates that our network learns a family of optimization criteria that selects informative points from the cloud. Our second experiment illustrates the robustness of our network, as explained in Thm 2.

Point Function Visualization As discussed in Sec 4.2, our network computes K (we take $K = 1024$ in this experiment) dimension point features for each point and aggregates all the per-point local features via a max pooling layer into a single K-dim vector, which forms the global shape descriptor.

To gain more insights on what the learnt per-point functions h's detect, we visualize the points p_i's that give high per-point function value $f(p_i)$ in Fig 7. This visualization clearly shows that different point functions

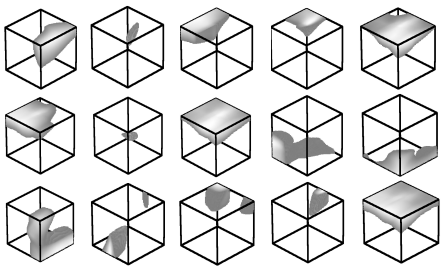

Figure 7. Point function visualization. For each per-point function h, we calculate the values $h(p)$ for all the points p in a cube of diameter two located at the origin, which spatially covers the unit sphere to which our input shapes are normalized when training our PointNet. In this figure, we visualize all the points p that give $h(p) > 0.5$ with function values color-coded by the brightness of the voxel. We randomly pick 15 point functions and visualize the activation regions for them.

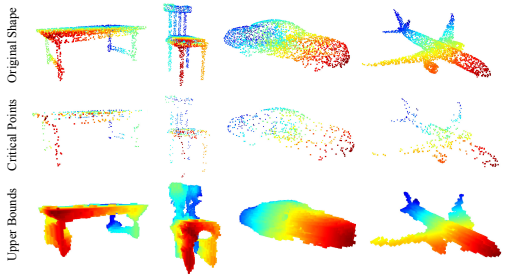

Figure 8. Critical points and upper bound shape. We visualize the critical points sets (the second row) and the upper bound shapes (the third row) for four query shapes listed in the first row. While the critical points jointly determine the global shape feature for the given shape, any point cloud that falls between the critical points set and the upper bound shape gives the exactly same feature. We color-code all figures to show the depth information.

learn to detect for points in different regions with various shapes scattered in the whole space.

Global Feature Visualization We visualize the shape family, as discussed in Thm 2, including all the shapes between the *critical point set* $\mathcal{C}_S$ and the *upper-bound shape* $\mathcal{N}_S$ that gives the same global feature $f(S)$ with respect to a given shape S.

Fig 8 shows the *critical point sets* $\mathcal{C}_S$ and *upper-bound shapes* $\mathcal{N}_S$ for four selected shapes. The original input point clouds are rendered in the first row while the $\mathcal{C}_S$ and $\mathcal{N}_S$ for them are shown in the second and their rows respectively. The $\mathcal{C}_S$ for a given shape S includes the points from the original point cloud that activates some per-point function h_i's the most. The $\mathcal{N}_S$ is constructed by pushing all the points in a diameter-2 cube through the network and select the points p whose per-point function values $(h_1(p), h_2(p), \cdots, h_K(p))$ are no larger than the global shape descriptor. It is not hard to see that all the shapes S' that cover $\mathcal{C}_S$ and are contained by $\mathcal{N}_S$ give the exactly same global feature $f(S') = f(S)$. The transition shape family entails the robustness of the our PointNet, meaning that adding noisy jitterings or losing some non-critical points do not change the learnt shape signature and thus do not affect our classification or segmentation results.

6. Conclusion

In this work, we propose a novel deep neural network *PointNet* that directly consumes point cloud. Our network provides a unified approach to a number of 3D recognition tasks including object classification, part segmentation and semantic segmentation, while obtaining on par or better results than state of the arts on standard benchmarks. We also provide theoretical analysis and visualizations towards understanding of our network.

References

[1] I. Armeni, O. Sener, A. R. Zamir, H. Jiang, I. Brilakis, M. Fischer, and S. Savarese. 3d semantic parsing of large-scale indoor spaces. In *Proceedings of the IEEE International Conference on Computer Vision and Pattern Recognition*, 2016.

[2] M. Aubry, U. Schlickewei, and D. Cremers. The wave kernel signature: A quantum mechanical approach to shape analysis. In *Computer Vision Workshops (ICCV Workshops), 2011 IEEE International Conference on*, pages 1626–1633. IEEE, 2011.

[3] M. M. Bronstein and I. Kokkinos. Scale-invariant heat kernel signatures for non-rigid shape recognition. In *Computer Vision and Pattern Recognition (CVPR), 2010 IEEE Conference on*, pages 1704–1711. IEEE, 2010.

[4] J. Bruna, W. Zaremba, A. Szlam, and Y. LeCun. Spectral networks and locally connected networks on graphs. *arXiv preprint arXiv:1312.6203*, 2013.

[5] D.-Y. Chen, X.-P. Tian, Y.-T. Shen, and M. Ouhyoung. On visual similarity based 3d model retrieval. In *Computer graphics forum*, volume 22, pages 223–232. Wiley Online Library, 2003.

[6] Y. Fang, J. Xie, G. Dai, M. Wang, F. Zhu, T. Xu, and E. Wong. 3d deep shape descriptor. In *Proceedings of the IEEE Conference on Computer Vision and Pattern Recognition*, pages 2319–2328, 2015.

[7] M. Gschwandtner, R. Kwitt, A. Uhl, and W. Pree. BlenSor: Blender Sensor Simulation Toolbox Advances in Visual Computing. volume 6939 of *Lecture Notes in Computer Science*, chapter 20, pages 199–208. Springer Berlin / Heidelberg, Berlin, Heidelberg, 2011.

[8] K. Guo, D. Zou, and X. Chen. 3d mesh labeling via deep convolutional neural networks. *ACM Transactions on Graphics (TOG)*, 35(1):3, 2015.

[9] M. Jaderberg, K. Simonyan, A. Zisserman, et al. Spatial transformer networks. In *NIPS 2015*.

[10] A. E. Johnson and M. Hebert. Using spin images for efficient object recognition in cluttered 3d scenes. *IEEE Transactions on pattern analysis and machine intelligence*, 21(5):433–449, 1999.

[11] M. Kazhdan, T. Funkhouser, and S. Rusinkiewicz. Rotation invariant spherical harmonic representation of 3 d shape descriptors. In *Symposium on geometry processing*, volume 6, pages 156–164, 2003.

[12] Y. Li, S. Pirk, H. Su, C. R. Qi, and L. J. Guibas. Fpnn: Field probing neural networks for 3d data. *arXiv preprint arXiv:1605.06240*, 2016.

[13] H. Ling and D. W. Jacobs. Shape classification using the inner-distance. *IEEE transactions on pattern analysis and machine intelligence*, 29(2):286–299, 2007.

[14] J. Masci, D. Boscaini, M. Bronstein, and P. Vandergheynst. Geodesic convolutional neural networks on riemannian manifolds. In *Proceedings of the IEEE International Conference on Computer Vision Workshops*, pages 37–45, 2015.

[15] D. Maturana and S. Scherer. Voxnet: A 3d convolutional neural network for real-time object recognition. In *IEEE/RSJ International Conference on Intelligent Robots and Systems*, September 2015.

[16] C. R. Qi, H. Su, M. Nießner, A. Dai, M. Yan, and L. Guibas. Volumetric and multi-view cnns for object classification on 3d data. In *Proc. Computer Vision and Pattern Recognition (CVPR), IEEE*, 2016.

[17] R. B. Rusu, N. Blodow, and M. Beetz. Fast point feature histograms (fpfh) for 3d registration. In *Robotics and Automation, 2009. ICRA'09. IEEE International Conference on*, pages 3212–3217. IEEE, 2009.

[18] R. B. Rusu, N. Blodow, Z. C. Marton, and M. Beetz. Aligning point cloud views using persistent feature histograms. In *2008 IEEE/RSJ International Conference on Intelligent Robots and Systems*, pages 3384–3391. IEEE, 2008.

[19] M. Savva, F. Yu, H. Su, M. Aono, B. Chen, D. Cohen-Or, W. Deng, H. Su, S. Bai, X. Bai, et al. Shrec16 track large-scale 3d shape retrieval from shapenet core55.

[20] H. Su, S. Maji, E. Kalogerakis, and E. G. Learned-Miller. Multi-view convolutional neural networks for 3d shape recognition. In *Proc. ICCV, to appear*, 2015.

[21] J. Sun, M. Ovsjanikov, and L. Guibas. A concise and provably informative multi-scale signature based on heat diffusion. In *Computer graphics forum*, volume 28, pages 1383–1392. Wiley Online Library, 2009.

[22] O. Vinyals, S. Bengio, and M. Kudlur. Order matters: Sequence to sequence for sets. *arXiv preprint arXiv:1511.06391*, 2015.

[23] D. Z. Wang and I. Posner. Voting for voting in online point cloud object detection. *Proceedings of the Robotics: Science and Systems, Rome, Italy*, 1317, 2015.

[24] Z. Wu, R. Shou, Y. Wang, and X. Liu. Interactive shape co-segmentation via label propagation. *Computers Graphics*, 38:248 – 254, 2014.

[25] Z. Wu, S. Song, A. Khosla, F. Yu, L. Zhang, X. Tang, and J. Xiao. 3d shapenets: A deep representation for volumetric shapes. In *Proceedings of the IEEE Conference on Computer Vision and Pattern Recognition*, pages 1912–1920, 2015.

[26] L. Yi, V. G. Kim, D. Ceylan, I.-C. Shen, M. Yan, H. Su, C. Lu, Q. Huang, A. Sheffer, and L. Guibas. A scalable active framework for region annotation in 3d shape collections. *SIGGRAPH Asia*, 2016.